Numerical experiences with Taylor methods

Carles Simó

Dept. Matemàtica Aplicada i Anàlisi, UB

Geometric Integration Conference

Universitat Jaume I

Castelló, 0609220930

Boundaries of stability

Consider a **totally elliptic** fixed point of an **autonomous Hamiltonian system or a symplectic map**. It is **linearly stable** if the eigenvalues are simple.

Questions:

a) What about **non linear stability**? In general not true for **3 or more degrees of freedom (DOF)**. There is no way to avoid **Arnol'd diffusion** (except in simple cases when some **Dirichlet-like theorem** applies). But perhaps one can talk about **practical stability** in some sense (mild diffusion in very long time intervals).

b) Up to which distance **there is stability in some sense**? Which **objects** appear at the **stability boundaries** (perhaps in a **weak or practical** sense).

c) How do the results depend on **parameters**?

These are **global** questions. Require use of **analytics** and **numerics**.

A toy problem: the Hénon map

Any quadratic area preserving map can be reduced to

$$\begin{pmatrix} x \\ y \end{pmatrix} \to \begin{pmatrix} x_1 \\ y_1 \end{pmatrix} = \begin{pmatrix} c(1-x^2)+2x+y \\ -x \end{pmatrix} \qquad x, y, c \in \mathbb{R}.$$

With this normalisation **fixed points** at H$=(-1,1)$ and E$=(1,-1)$.

Last one **elliptic** if $c \in [0,2]$. A **Normal Form** analysis proves **non linear stability** if $c \in (0,2) \setminus \{1.5\}$.

A **global stability** criterion: Points which do not escape to infinity.

Relevant comment: In this toy problem (equivalent to a Poincaré map of a 2DOF Hamiltonian) there are domains of **true stability** due to **KAM theorem**.

Let us scan the domain $[-1,2.1]\times[-1,2.1]$ with step size 0.001 and keep the non escaping points. All points outside this domain escape. Different checks are done concerning criteria, number of iterates, etc.

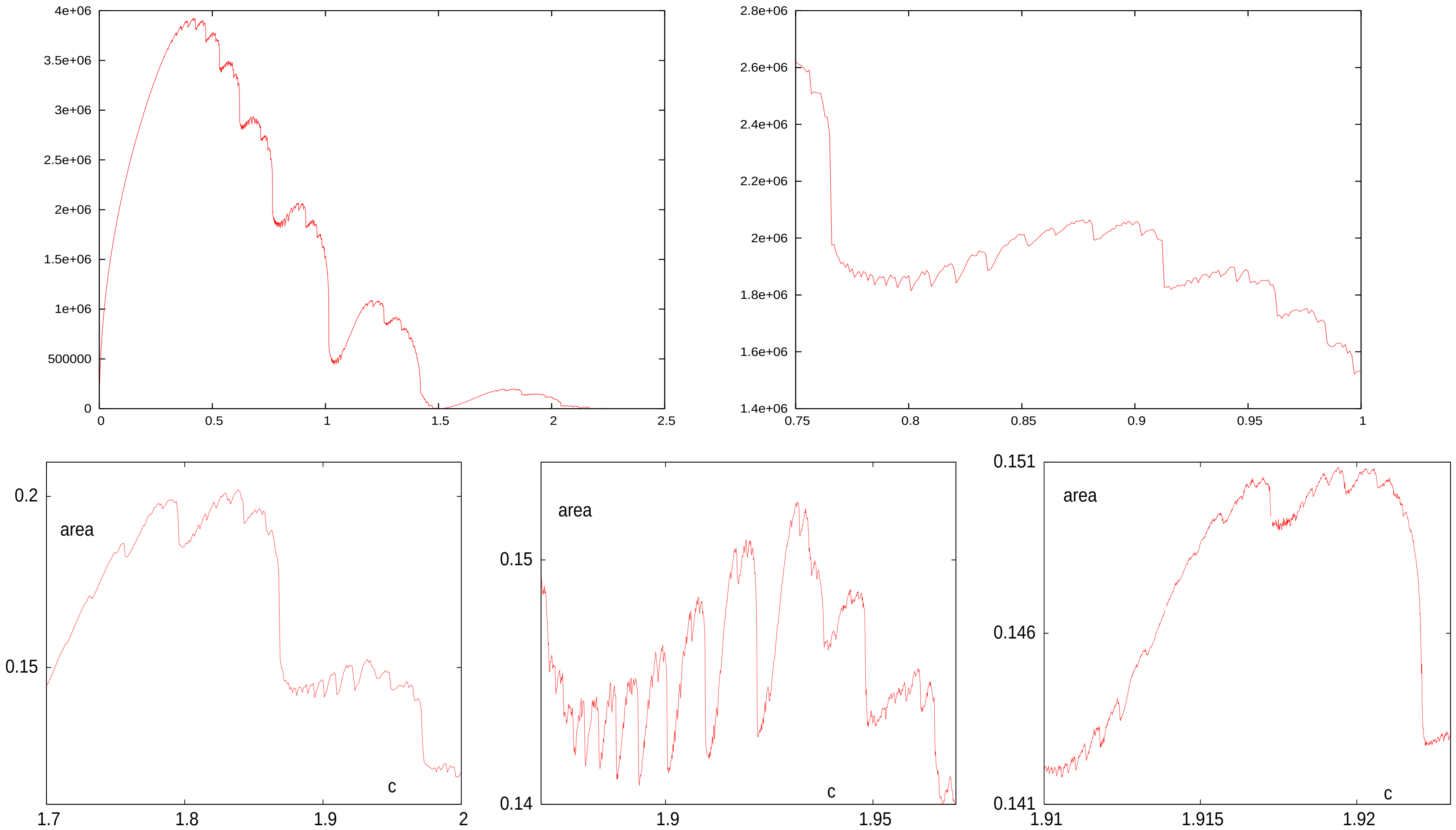

Statistics of results and some details.

The ultimate boundaries to confine motion are the invariant manifolds of H. But for some escaping points it can be necessary a large number of iterations to reach a small nbd of H.

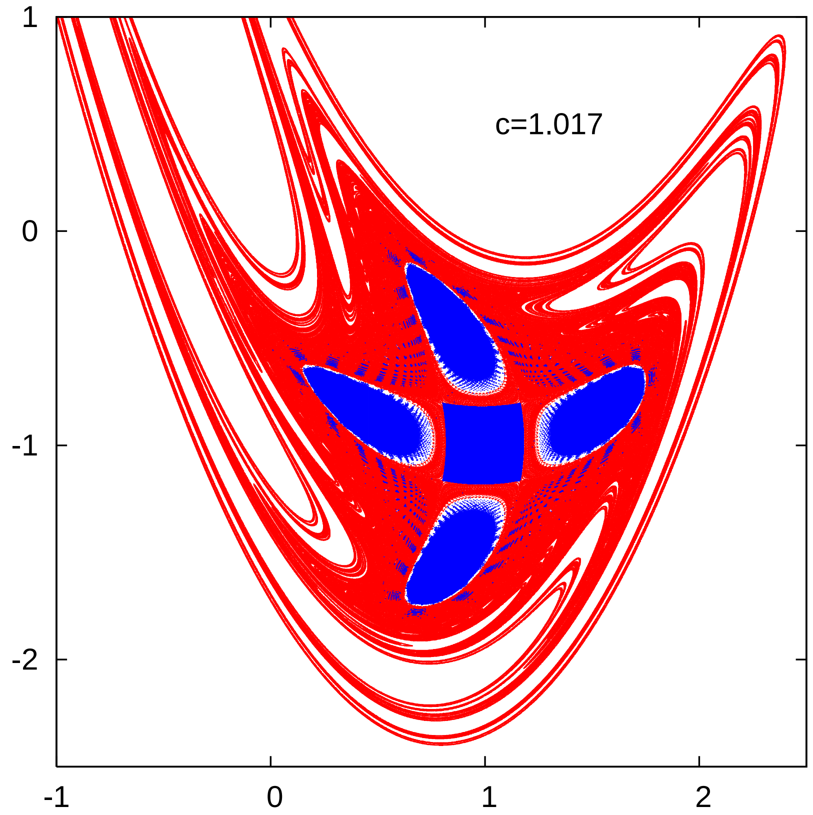

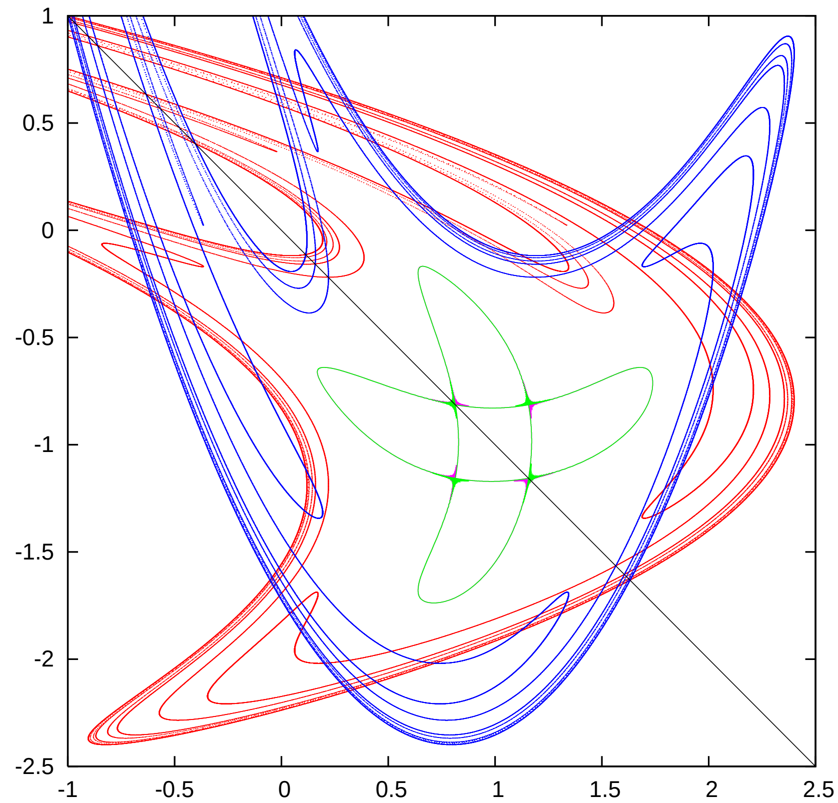

Left: Points in W^s_H (red) and non escaping (blue) for $c = 1.017$. Right: Manifolds of H (W^s_H in blue, W^u_H in red) and of the hyperbolic period-4 orbit (in magenta and green, resp.) for $c = 1.015$. Note that red and green finally connect.

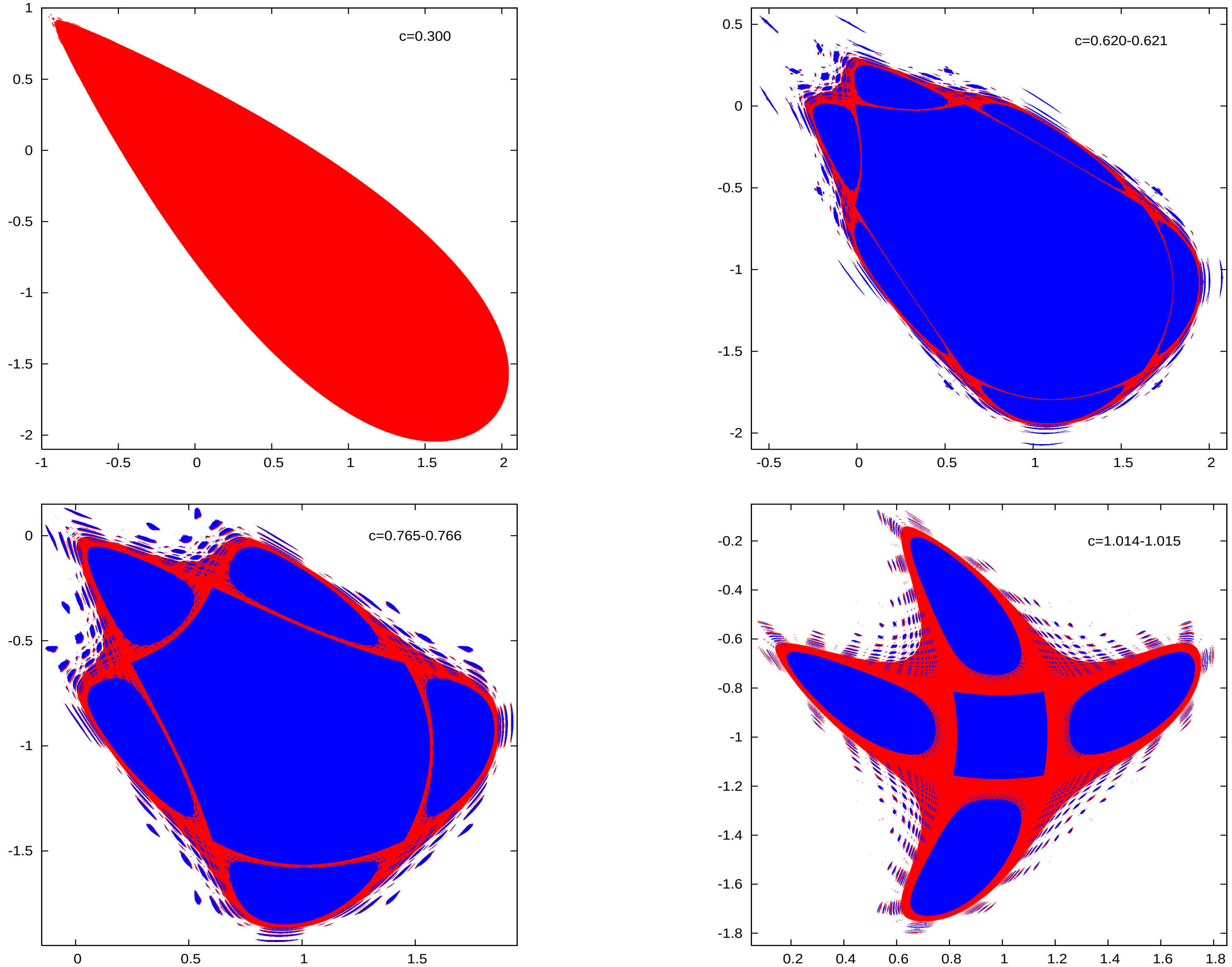

Examples of the results for selected c and transitions.

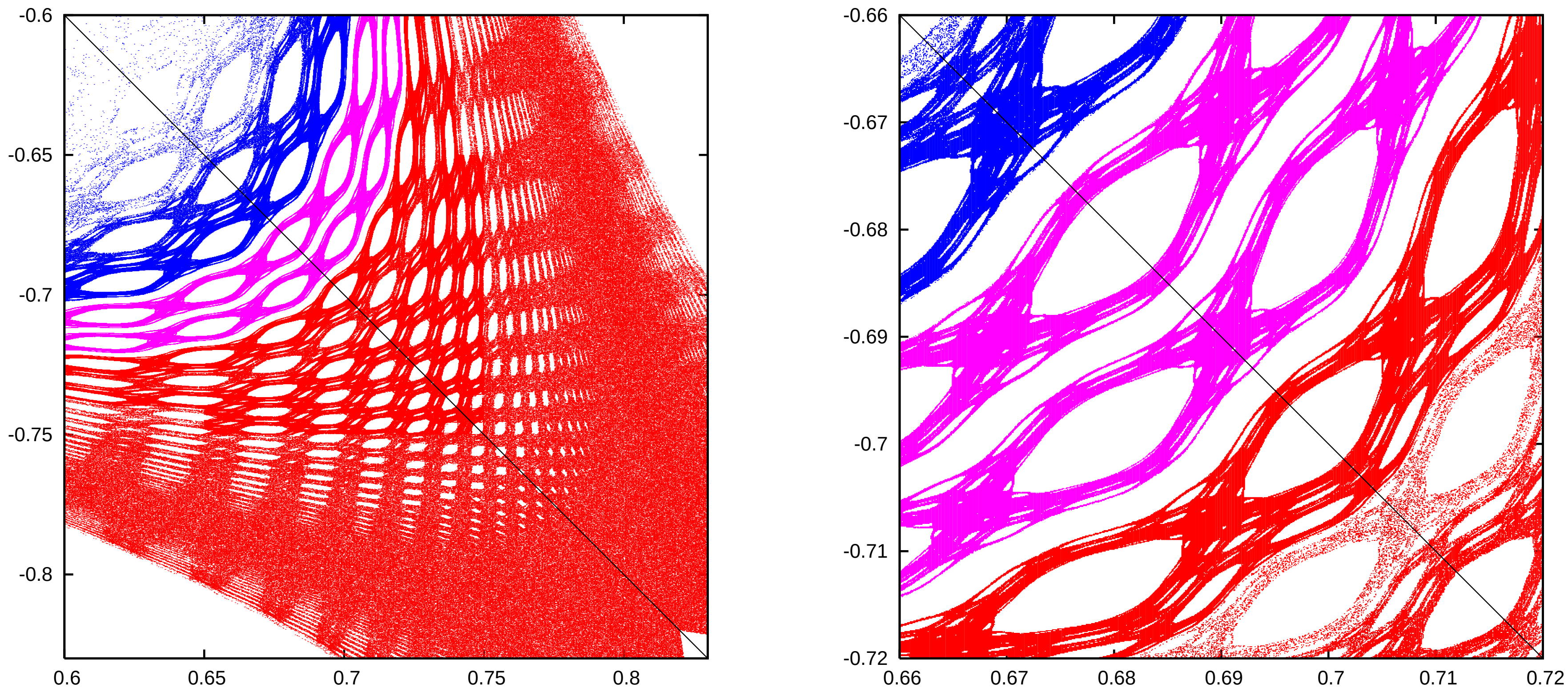

Magnifications of a region close to $y = -x$ for $c = 1.0141$. Points in red, blue, correspond to single orbits. Points in magenta correspond to two orbits, one in each domain. One can see the negative of the islands. Only points in blue escape, but for $c = 1.0142$ all these points escape. For $c = 1.0141$ there are three gaps candidate to contain invariant (rotational) curves.

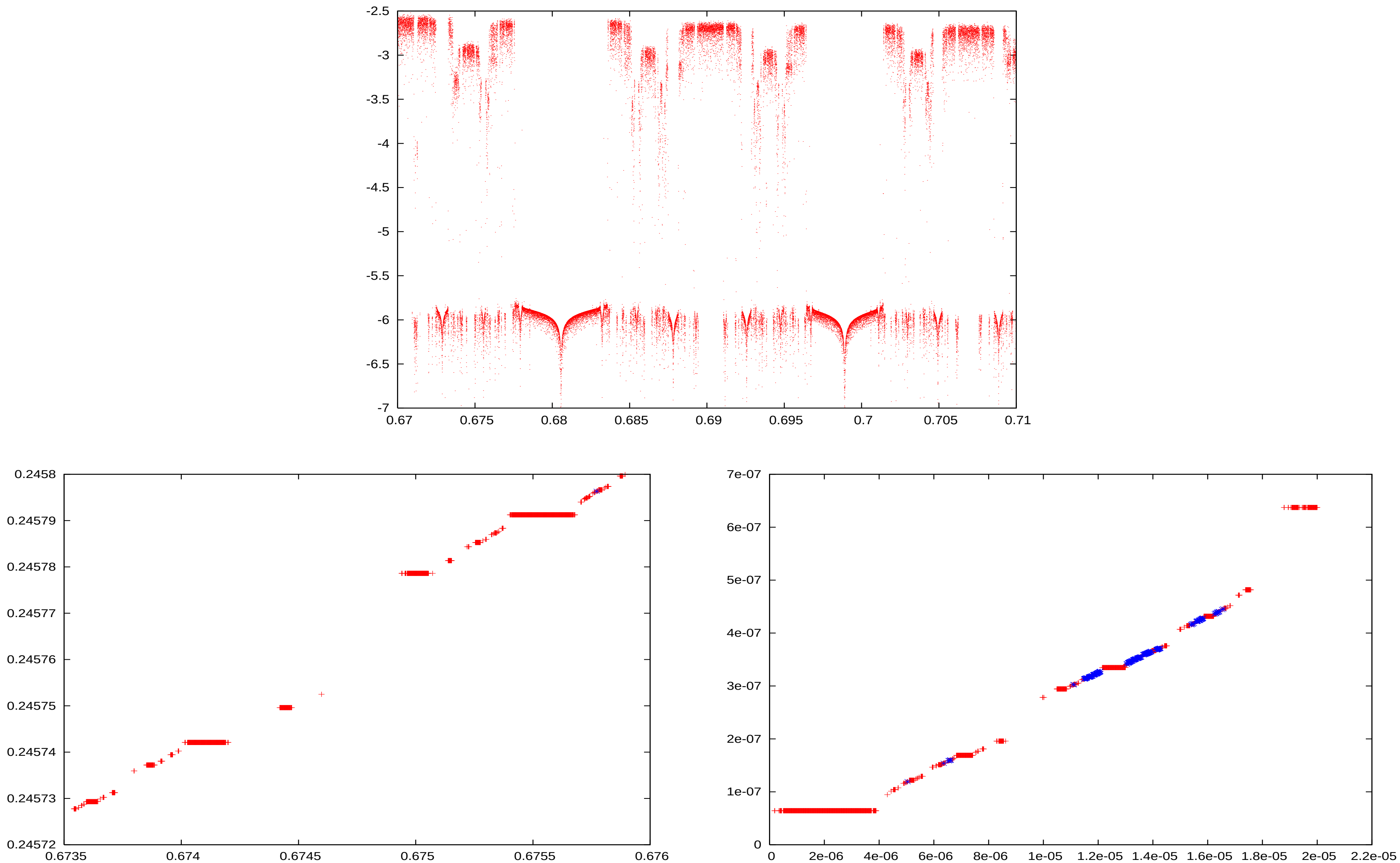

Lyapunov exponent (in $\log_{10}$) and rotation number for selected decreasing intervals. In blue candidates to invariant curve (not well approximated by rationals with denominator less than 10^7).

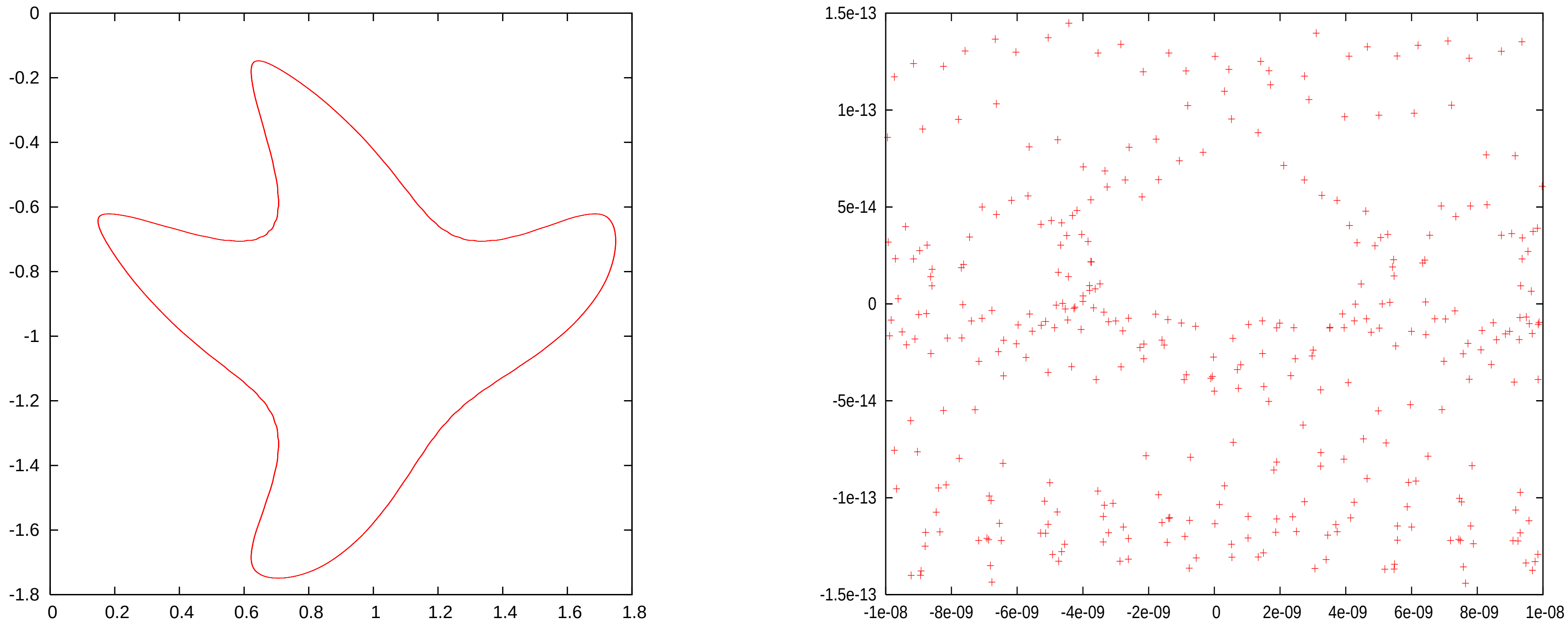

Left: What seems to be an invariant curve for $c = 1.0141$ passing through $x_0 = -y_0 = 0.6757666$. Right: Iterates with $|x - x_0| < 10^{-8}$ among the first 10^{10} iterates, after the affinity $(x, y) \mapsto (x - x_0, y - x + 2x_0)$ and subtracting a quadratic fit. Width of the cloud of points: 3×10^{-13}.

What about theoretical proofs?

Of course, these numerical experiments prove nothing in the mathematical sense, but give good hints about the location of curves close to the last invariant curve.

To convert these results into a proof one needs

- Concerning the invariant curve: To produce a Fourier approximation of the invariant curve, to obtain a normal form around it with rigorous estimate of the remainder and to apply KAM theory.
- Concerning the existence of nearby points which escape: To find a heteroclinic chain of transversal intersections with initial manifold close to the invariant curve and with final manifold the one of the H point.

Both computations have to be done using interval arithmetic (or any other method giving rigorous estimates) and require a finite (may be long) number of computations (may be multiple precision).

This kind of **CAP** (Computer Assisted Proof) is feasible in both cases with the methods known at present.

Taylor integration method

Consider an IVP for an ODE like

$$\dot{x} = f(t, x), \qquad x(t_0) = x_0,$$

where f is assumed to be analytic in a nbd of $(t_0, x_0) \in \Omega \subset \mathbb{R} \times \mathbb{R}^n$.

We want to produce in an easy way the Taylor expansion $x(t_0 + h)$ for suitable values of h and use it as a one-step method.

For a very large class of functions the evaluation of f can be split in simple expressions

$$\begin{aligned}
e_1 &= g_1(t, x), \\
e_2 &= g_2(t, x, e_1), \\
&\vdots \\
e_j &= g_j(t, x, e_1, \ldots, e_{j-1}), \\
&\vdots \\
e_m &= g_m(t, x, e_1, \ldots, e_{m-1}), \\
f_1(t, x) &= e_{k_1}, \\
&\vdots \\
f_n(t, x) &= e_{k_n},
\end{aligned}$$

where each one of the expressions e_j contains a sum of arguments, a product or quotient of two arguments or an elementary function (like sin, cos, log, exp, $\sqrt{,}\ldots$) of a single argument.
The basic idea is to compute in a recurrent way the power series expansion of all the e_j. All the g_j have to be seen as operations with (truncated) power series. The input are t and the coefficients of order 0 of the components of x_0. At the end of first step we know the terms of order 1 of these components. If the terms up to order s of the arguments of the g_j are known, we obtain easily the coefficient of order s of e_j.
Hence the representation of the components x_i of $x(t_0 + h)$ looks like

$$x_i = \sum_{s=0}^{N} a_i^{(s)} h^s.$$

There are several strategies to select order and step to have, approximately, some desired truncation error. Also to save computing time (like multiplying by a precomputed $1/s$ instead of dividing by s), but some caution is required to avoid systematic errors.

Some interesting properties

- Under reasonable conditions the optimal stepsize (concerning efficiency for fixed truncation error) is essentially independent of the number of digits used.
- The optimal order is approximately linear in the number of digits.
- The computational cost (measured in number of elementary operations) is approximately quadratic in the number of digits.

Some elementary pitfalls are shown in the next figures, for the integration of $\dot{x} = -y$, $\dot{y} = x$. The order used is $N = 24$, the local tolerance is 10^{-21} and the final time $2\pi \times 10^9$. Different runs use multiplication by $1/s$ instead of division by s to obtain $a_i^{(s)}$ from some s_0 on. The plots show absolute errors in energy as a function of t and the average slope of the energy as a function of t, both for several values of s_0.

It is also convenient to use truncation errors small compared to the ε of the processor, to avoid biases.

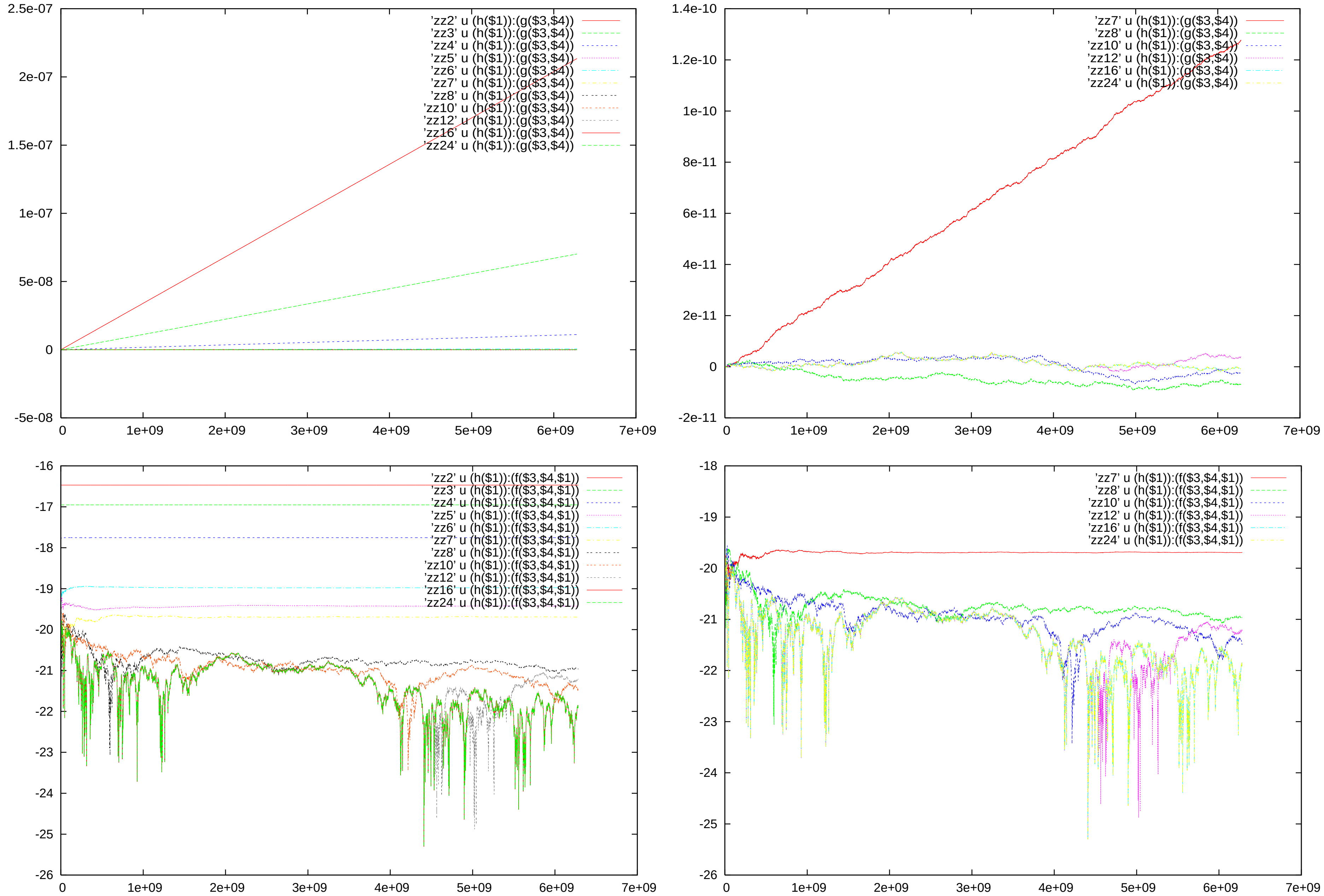

'zz2' u (h($1)):(g($3,$4))
'zz3' u (h($1)):(g($3,$4))
'zz4' u (h($1)):(g($3,$4))
'zz5' u (h($1)):(g($3,$4))
'zz6' u (h($1)):(g($3,$4))
'zz7' u (h($1)):(g($3,$4))
'zz8' u (h($1)):(g($3,$4))
'zz10' u (h($1)):(g($3,$4))
'zz12' u (h($1)):(g($3,$4))
'zz16' u (h($1)):(g($3,$4))
'zz24' u (h($1)):(g($3,$4))
'zz2' u (h($1)):(f($3,$4,$1))
'zz3' u (h($1)):(f($3,$4,$1))
'zz4' u (h($1)):(f($3,$4,$1))
'zz5' u (h($1)):(f($3,$4,$1))
'zz6' u (h($1)):(f($3,$4,$1))
'zz7' u (h($1)):(f($3,$4,$1))
'zz8' u (h($1)):(f($3,$4,$1))
'zz10' u (h($1)):(f($3,$4,$1))
'zz12' u (h($1)):(f($3,$4,$1))
'zz16' u (h($1)):(f($3,$4,$1))
'zz24' u (h($1)):(f($3,$4,$1))
0
1e+09
2e+09
3e+09
4e+09
5e+09
6e+09
7e+09

Stability of the planar circular RTBP for outer motion

Next we consider a problem similar to the Hénon map, but requiring numerical integration: The planar circular RTBP which describes the motion of a massless particle (think about an asteroid) under the gravitational attraction of two primaries (think about Sun and Jupiter) moving in circular orbit about their center of masses. The mass ratio of the system is $\mu = m_J/(m_S + m_J)$.

The system has a first integral known as Jacobi integral C. For large enough values of C the level of this function has 3 connected components: Two close to the primaries and the third one away from them. Motion in this outer region corresponds to bodies with perihelion at a distance larger than the Sun-Jupiter distance.

If we neglect the effect of Jupiter the motion of the massless body will be a two-body motion around the Sun. If we fix e=eccentricity (the so-called osculating eccentricity) then C determines the value of the semiaxis a.

Theorem (V. Kaloshin et al, 2006, in preparation)
Given μ and $C > C_0$ there exist $e_0(\mu, C)$ such that if $e > e_0$ there are bodies with initial osculating eccentricity e which escape to infinity.

For $\mu = 10^{-3}$, $C = 3.6$ the estimated value of e_0 is 0.75. Proof and application are based on Aubry-Mather theory.

Next figures show orbits of different initial points on the Poincaré section corresponding to pericenter passages.

Top left: e as a function of $q = a(1 - e)$ for $\mu = 0$. Top right: images of several initial conditions. For $q < 1.742$ (and, probably, $q < 1.748$) there are points in a chaotic zone which can escape. For $q > 1.750$ points seems definitely that do not escape because of the existence of invariant curves. Bottom figures show magnifications. In blue a set of invariant curves.
In the next page the curves are shown alone. For one located at the bottom (with initial $q = 1.74946$, leaving orthogonally from x axis), the iterates following on a narrow window and how they occur as a function of the number of iterates in the window are shown. Final time 11.25×10^7 Jupiter revolutions.

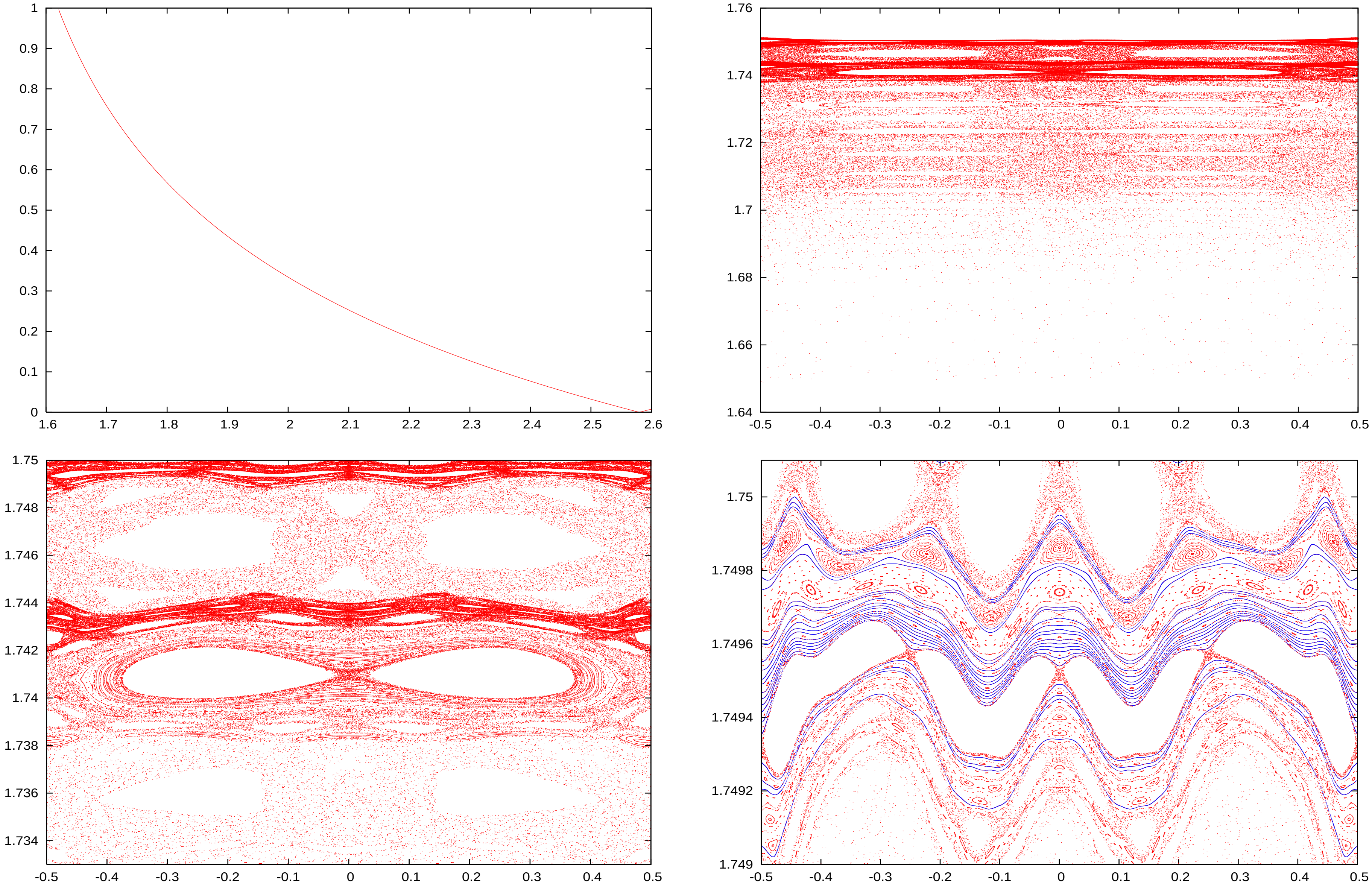

1
0.9
0.8
0.7
0.6
0.5
0.4
0.3
0.2
0.1
0
1.6
1.7
1.8
1.9
2
2.1
2.2
2.3
2.4
2.5
2.6
1.76
1.74
1.72
1.7
1.68
1.66
1.64
-0.5
-0.4
-0.3
-0.2
-0.1
0
0.1
0.2
0.3
0.4
0.5
1.75
1.748
1.746
1.744
1.742
1.74
1.738
1.736
1.734
1.75
1.7498
1.7496
1.7494
1.7492
1.749

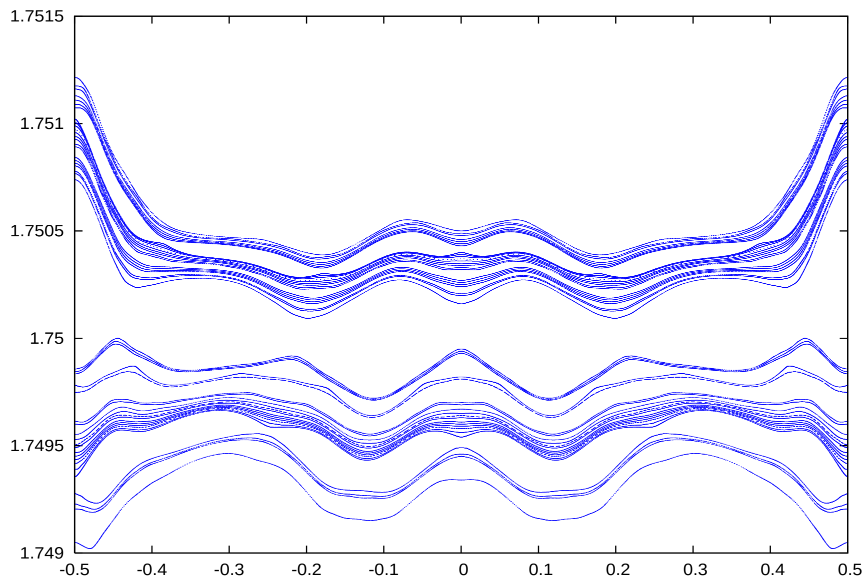

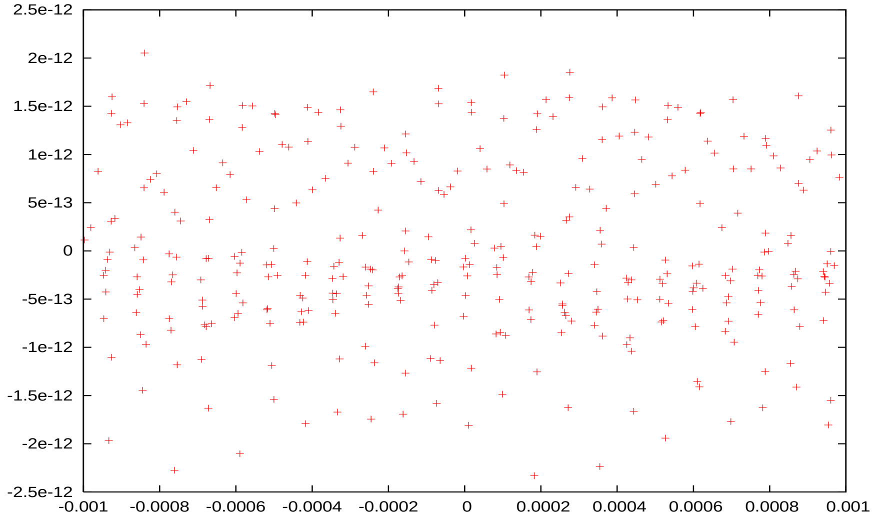

These results seem to support $0.652 < e_0 < 0.666$ for the chosen μ, C.

Stability of the triangular points in the circular 3D RTBP (Work in progress)

Known results

- They are linearly stable for the mass parameter $\mu \in [0, \mu_1]$, where

$$\mu_s = \omega_{\text{short}}/\omega_{\text{long}} = s, \qquad s \in \mathbb{N}.$$

$\omega_{\text{short}}, \omega_{\text{long}}$ = frequencies at $L_{4,5}$ in the 2D case. $\omega_z = 1$.

$$\left[(1 \pm (1 - 27\mu(1-\mu))^{1/2})/2\right]^{1/2}.$$

- Nonlinear stability for $\mu \in [0, \mu_1] \setminus \{\mu_2, \mu_3\}$ in the 2D case.
- The nonlinear stability of the spatial problem is unknown. Probably there is some amount of Arnol'd diffusion.
- There is a domain of "practical stability", around $L_{4,5}$, which is not too small.

  Let $H = H_2 + H_3 + \ldots$ be the Hamiltonian around $L_{4,5}$.

$$H_2 = \frac{1}{2}\omega_s(q_1^2 + p_1^2) - \frac{1}{2}\omega_l(q_2^2 + p_2^2) + \frac{1}{2}\omega_z(q_3^2 + p_3^2).$$

Compute NF up to a suitable order, assuming no resonance. Bound the remainder and its effect $|\dot{I}_j|$ on actions of the NF. Use linear combinations of the actions which define a convex set around the triangular points.

Given T and δ, there exists an initial radius, ρ_0, such that if $(Q,P)_{t=0} \in B_{\rho_0}$ then $(Q,P)_t \in B_{\rho_0(1+\delta)}$ for all $|t| < T$, where B_ρ denotes the ball of radius ρ centered at the origin. I.e. **practical or effective stability**.

As a result one obtains, in general, **explicit Nekhorosev type estimates** (i.e., for δ fixed, one has $T \approx \exp(c/\rho^d)$, for some positive constants c, d).

- Numerical simulations show a **large "stable domain"**.

The stability domain

Conditions to be satisfied:

a) Projection on (x, y) **not encircling the main primary**,

b) Not **too close approaches to primaries**,

c) Projection on (x, y) **not below some critical** y (e.g. $y_c = -0.5$).

d) Starting on **zero velocity surface**.

On the integration method

Integration of ODE is done using a **Taylor method**.

Numerical values of the coefficients computed by recurrence (automatic differentiation formulae) up to high order (e.g. order 24) and with time step such that the requested local error is below the ε of the processor (e.g. 10^{-21}).

Question What about **energy conservation**?

Long range integrations

For $\mu = 0.001$ a test on a sample of 175 i. c. as follows: $\Delta\rho = 0.0005$; $\alpha = 0.1\,(0.05)\,0.4$; $z = 0\,(0.2)\,0.8$, heliocentric, from a suitable origin of $\rho = R - 1$, α in revolutions. 75 points subsist for $t_{\text{final}} = 10^9$ Jupiter revolutions ($\approx$ **twice the age of Solar System**).

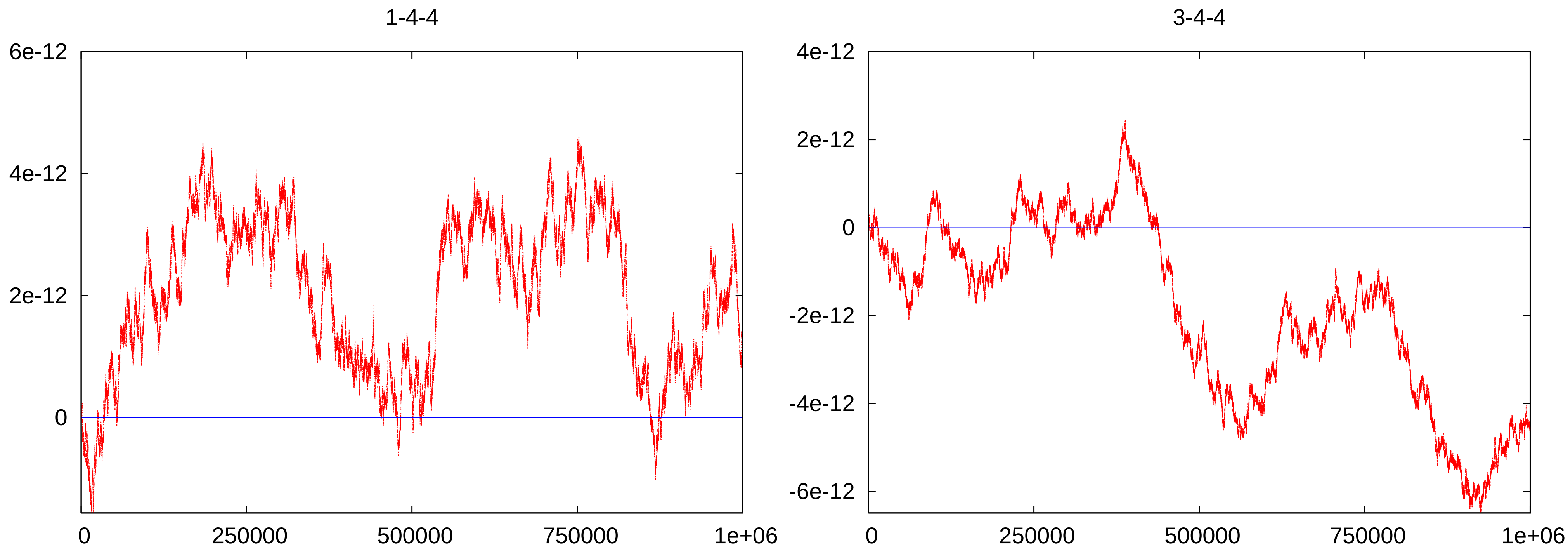

Shown: the 3 worst cases and the best one.

Errors w.r.t. initial energy displayed every 1000 Jupiter revolutions (J.r.).

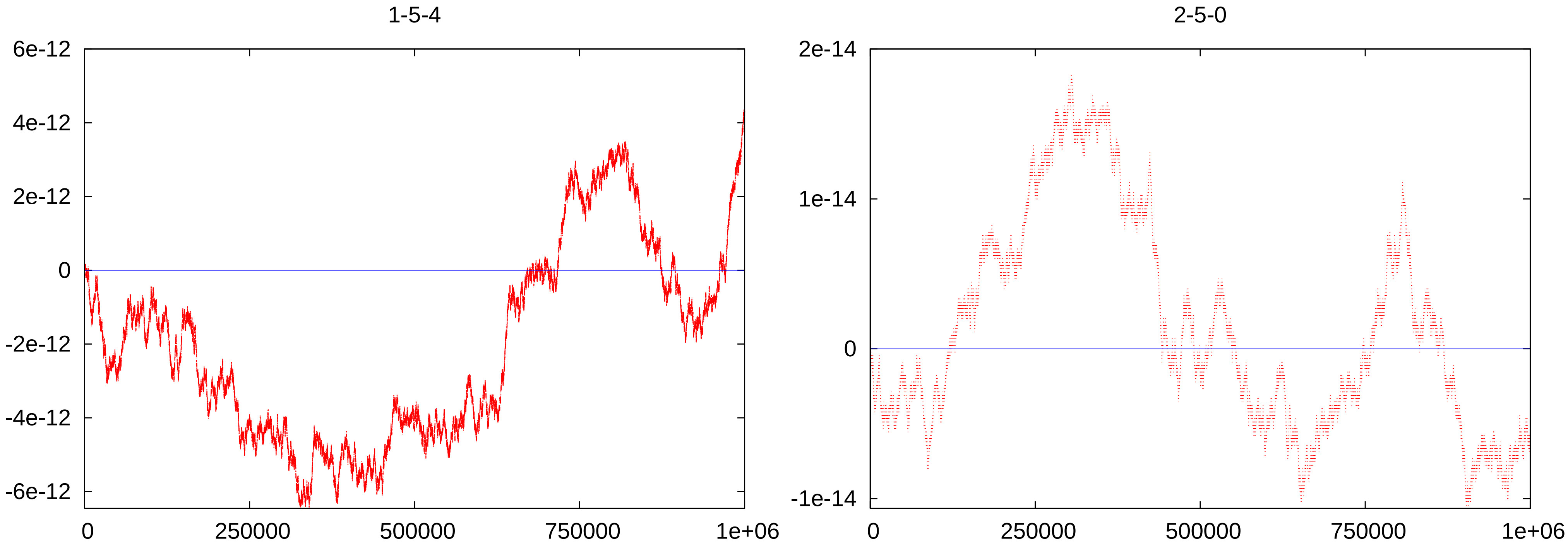

Average **integration step**: Worst case 0.36 years; best case 2.08 years.

Relevant statistics:

a) Histogram of **jumps of energy** every 1000 J.r. Unit: $2^{-52} \approx 2 \times 10^{-16}$,

b) **Maximal errors** and $1\,\sigma$ predicted values from previous plots,

c) **Autocorrelation** for the worst case.

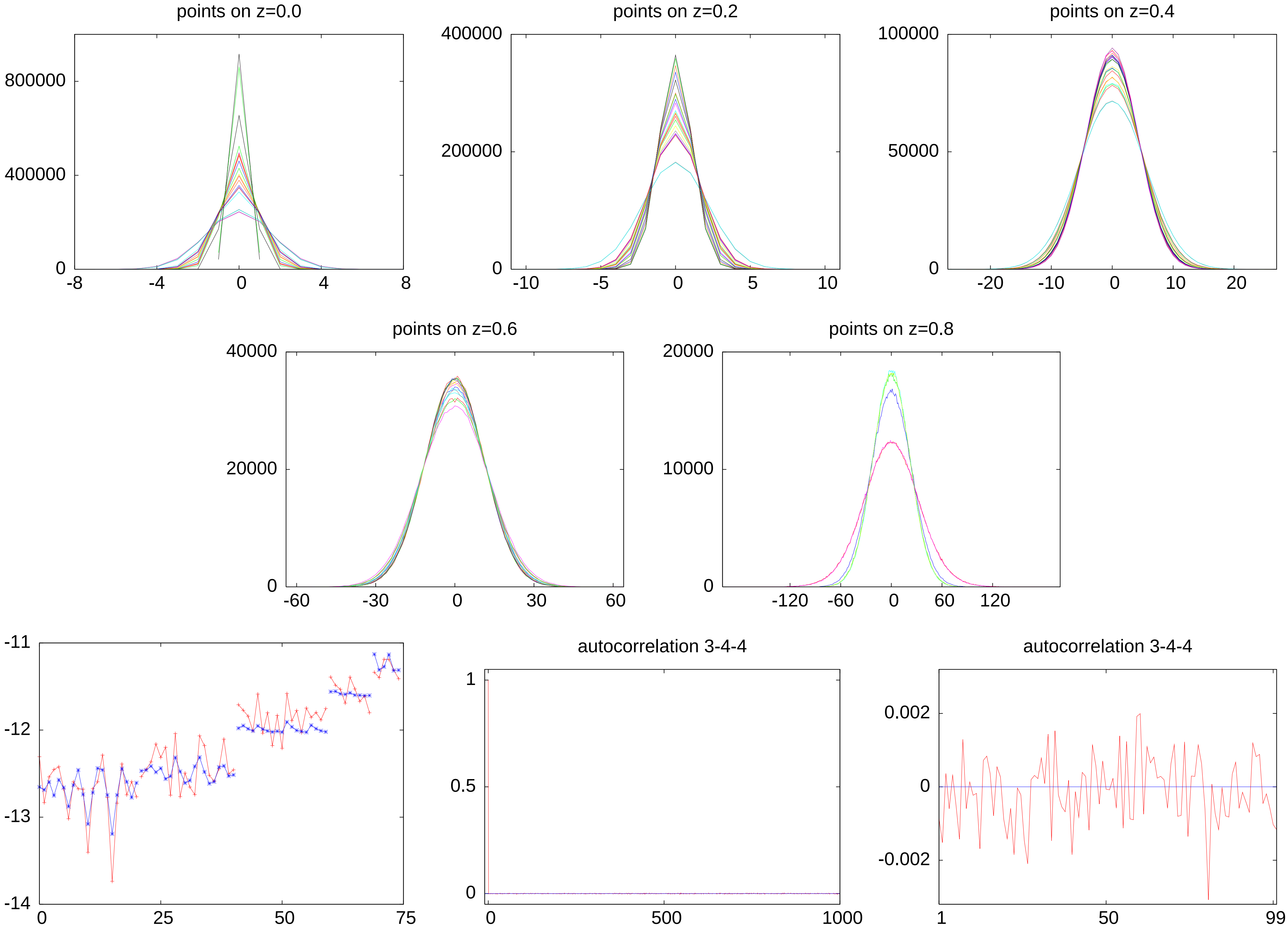
points on z=0.0
800000
400000
0
-8
-4
0
4
8
points on z=0.2
400000
200000
0
-10
-5
0
5
10
points on z=0.4
100000
50000
0
-20
-10
0
10
20
points on z=0.6
40000
20000
0
-60
-30
0
30
60
points on z=0.8
20000
10000
0
-120
-60
0
60
120
-11
-12
-13
-14
0
25
50
75
autocorrelation 3-4-4
1
0.5
0
0
500
1000
autocorrelation 3-4-4
0.002
0
-0.002
1
50
99

Preliminary results: Statistics

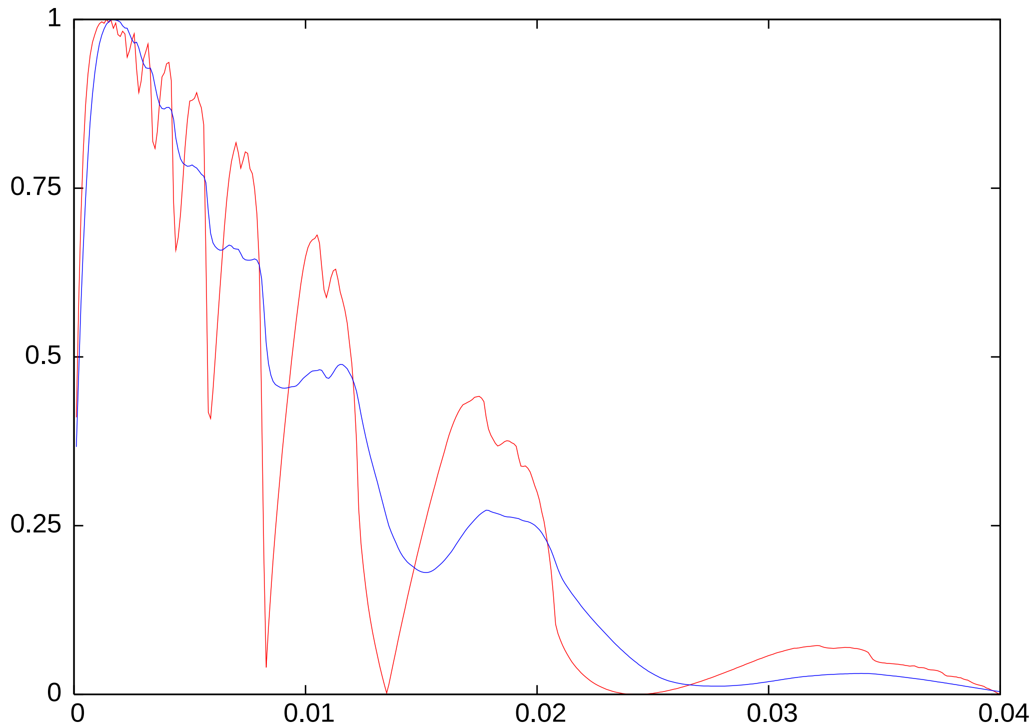

Normalized subsisting points. Planar case: $\Delta\rho = 10^{-4}$, $\Delta\alpha = 2 \times 10^{-4}$. Maximal value, for $\mu = 0.0014$, 282757 points. Spatial case: $\Delta\rho = 10^{-4}$, $\Delta\alpha = 5 \times 10^{-4}$, $\Delta z = 5 \times 10^{-3}$. Maximal value, for $\mu = 0.0017$, 19014882 points. Total scanned points: 8×10^{10}. Subsisting a first filter 2.17×10^{9}. The role of resonances is clearly seen (2D, 3D differ)

Spatial case being refined at present (completed 90%).

The case $\mu = 0$

For $\mu = 0$ one must be in $1-1$ resonance. Hence

$$z = \sqrt{\frac{4}{(1+R^2)^2} - R^2},$$

or

$$\psi = 1-\frac{1}{2}w+\frac{3}{2^5}w^2-\frac{1}{2^8}w^3-\frac{25}{2^{13}}w^4+\frac{33}{2^{16}}w^5+\frac{175}{2^{20}}w^6-\frac{497}{2^{23}}w^7-\frac{4401}{2^{29}}w^8+O(w^9),$$

where $w = z^2$, $\psi = \psi(z) = R^2$.

This suggests to plot $(\alpha,\ 1+\rho-\sqrt{\psi(z)},\ z)$.

Variables used for the representations: Cylindrical Heliocentric, with α in revolutions, $\rho = r_1 - 1$, z.

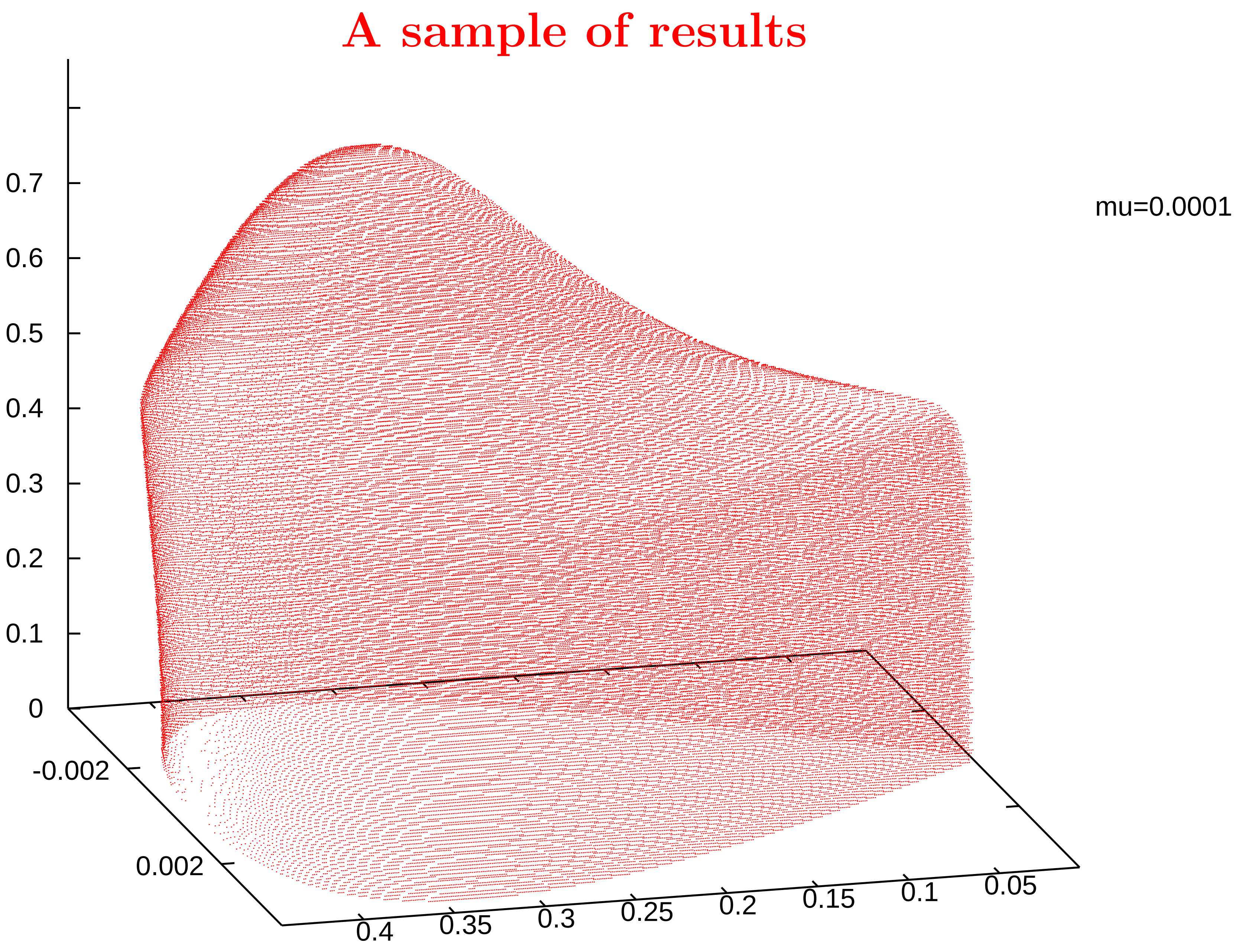
A sample of results
0.7
0.6
0.5
0.4
0.3
0.2
0.1
0
-0.002
0.002
0.4
0.35
0.3
0.25
0.2
0.15
0.1
0.05
mu=0.0001

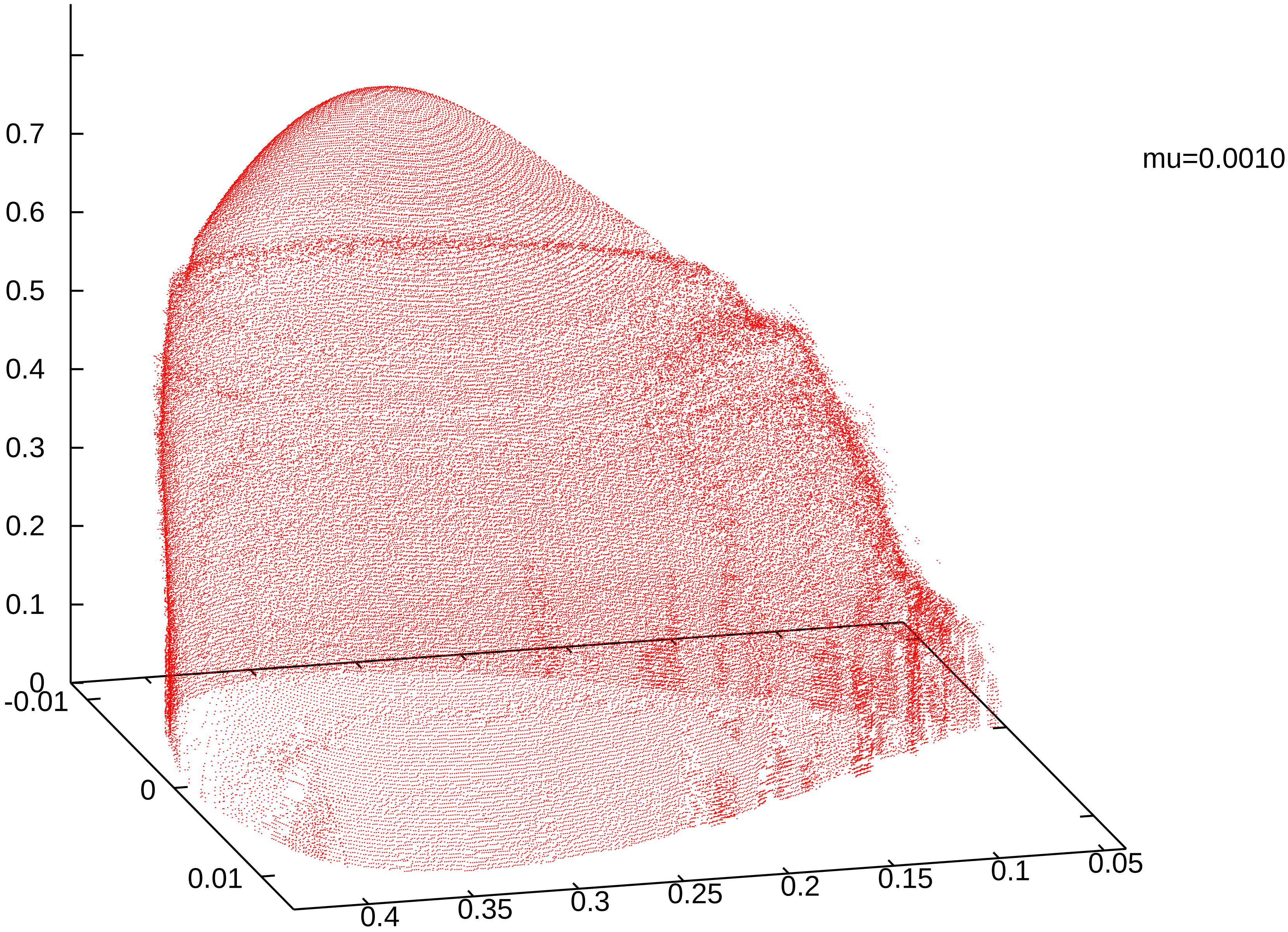

0.7
0.6
0.5
0.4
0.3
0.2
0.1
0
-0.01
0
0.01
0.4
0.35
0.3
0.25
0.2
0.15
0.1
0.05
mu=0.0010

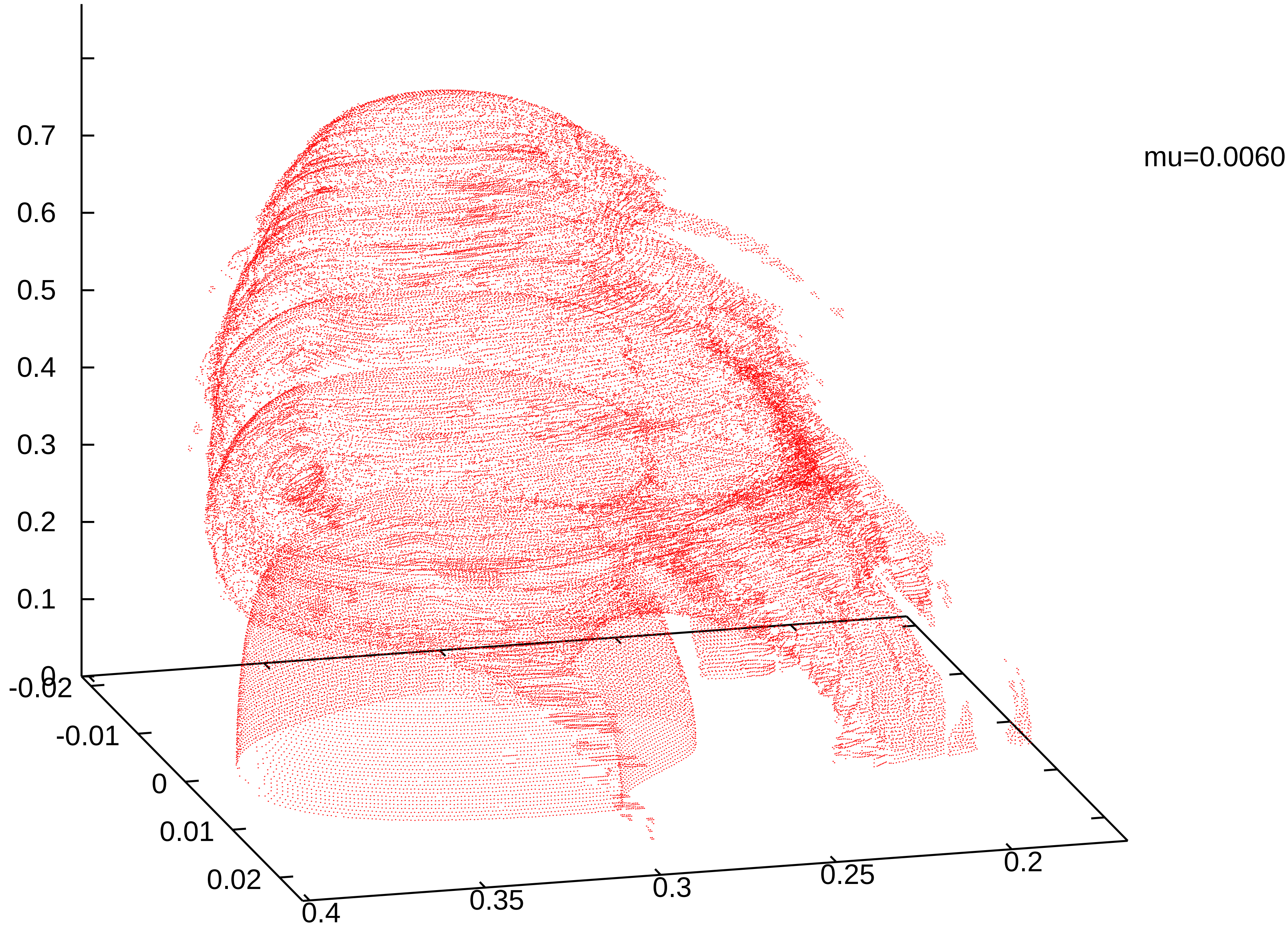

mu=0.0060
0.7
0.6
0.5
0.4
0.3
0.2
0.1
0
-0.02
-0.01
0
0.01
0.02
0.4
0.35
0.3
0.25
0.2

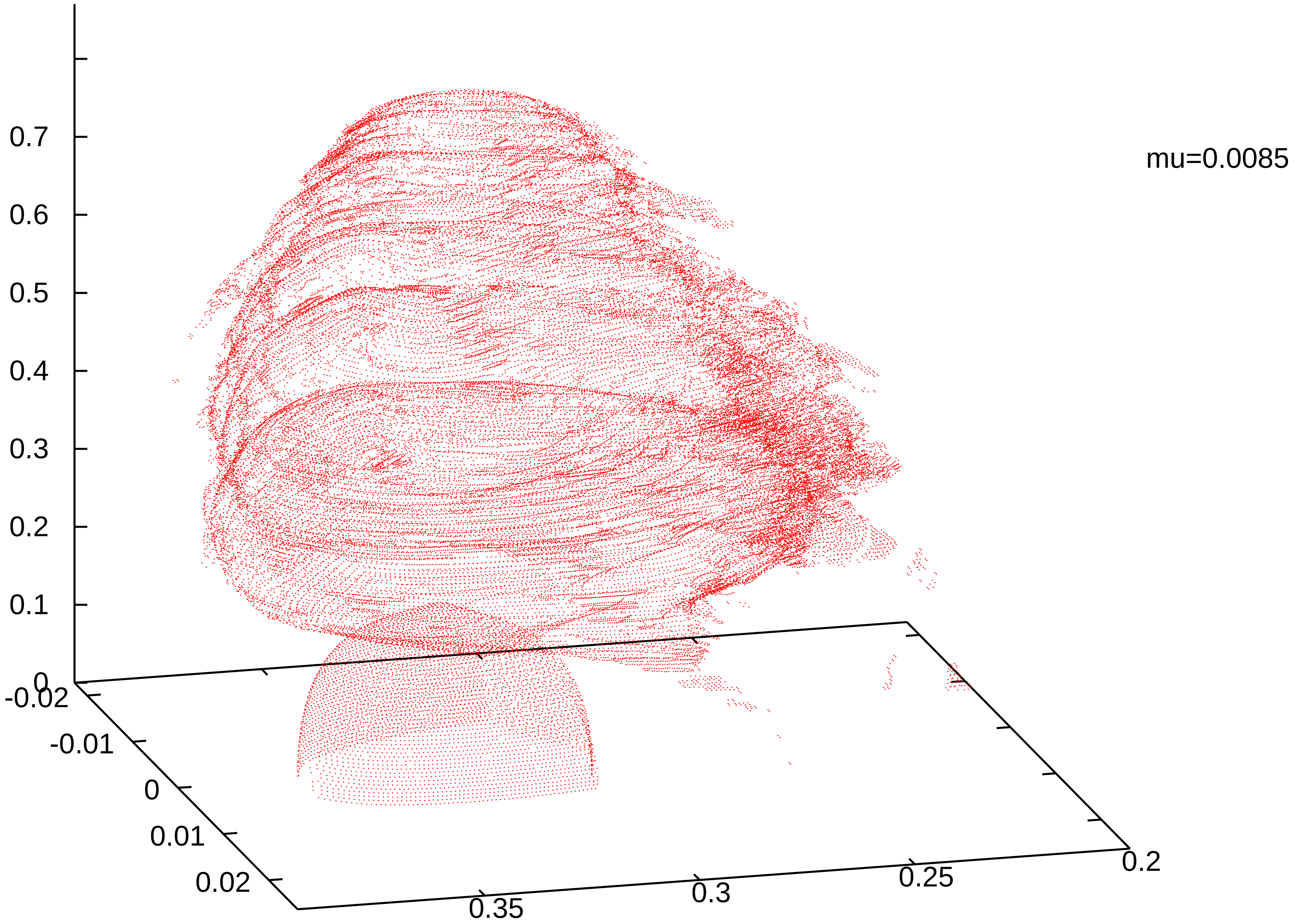

mu=0.0085
0.7
0.6
0.5
0.4
0.3
0.2
0.1
0
-0.02
-0.01
0
0.01
0.02
0.35
0.3
0.25
0.2

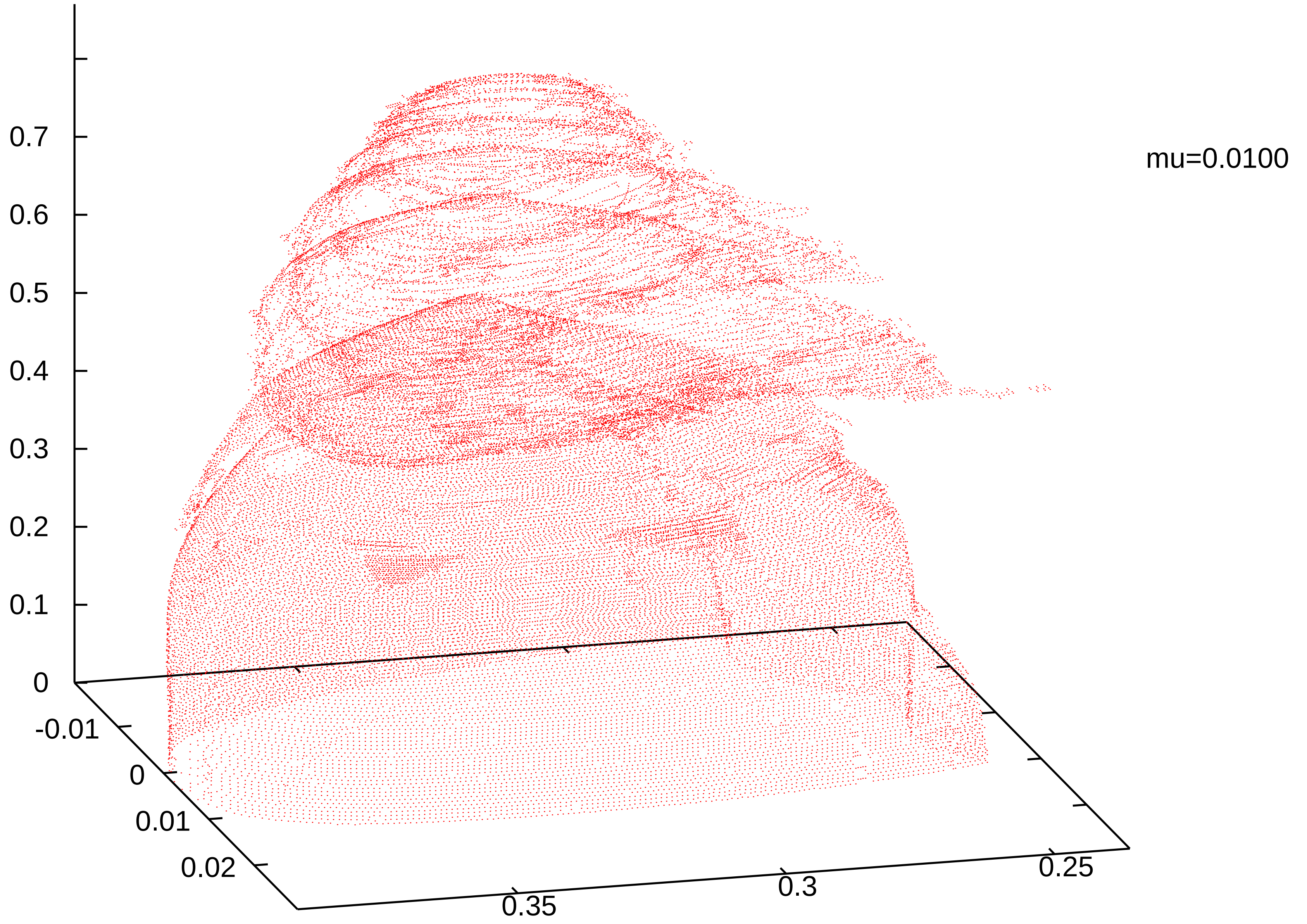

mu=0.0100
0.7
0.6
0.5
0.4
0.3
0.2
0.1
0
-0.01
0
0.01
0.02
0.35
0.3
0.25

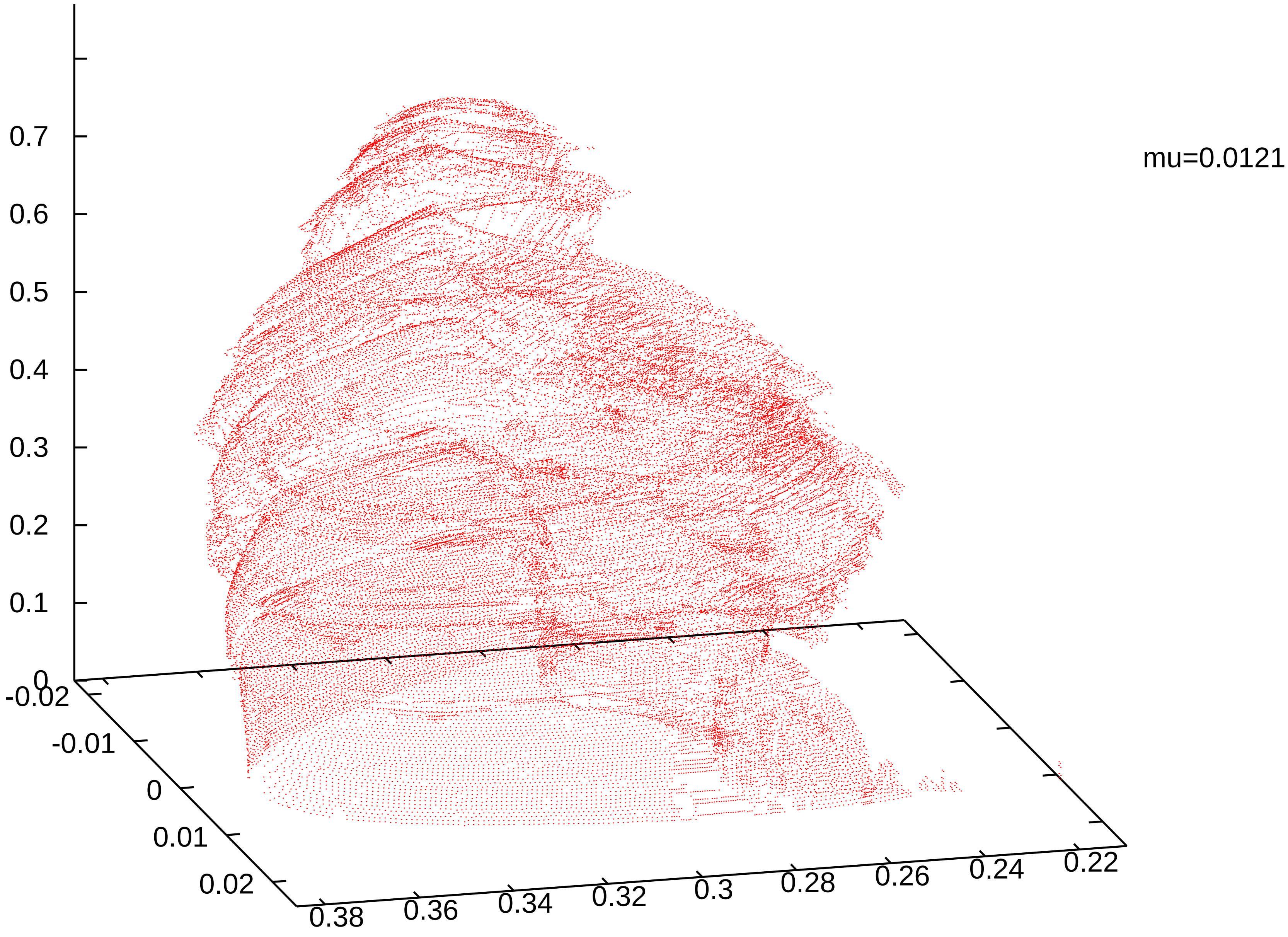

0.7
0.6
0.5
0.4
0.3
0.2
0.1
0
-0.02
-0.01
0
0.01
0.02
0.38
0.36
0.34
0.32
0.3
0.28
0.26
0.24
0.22
mu=0.0121

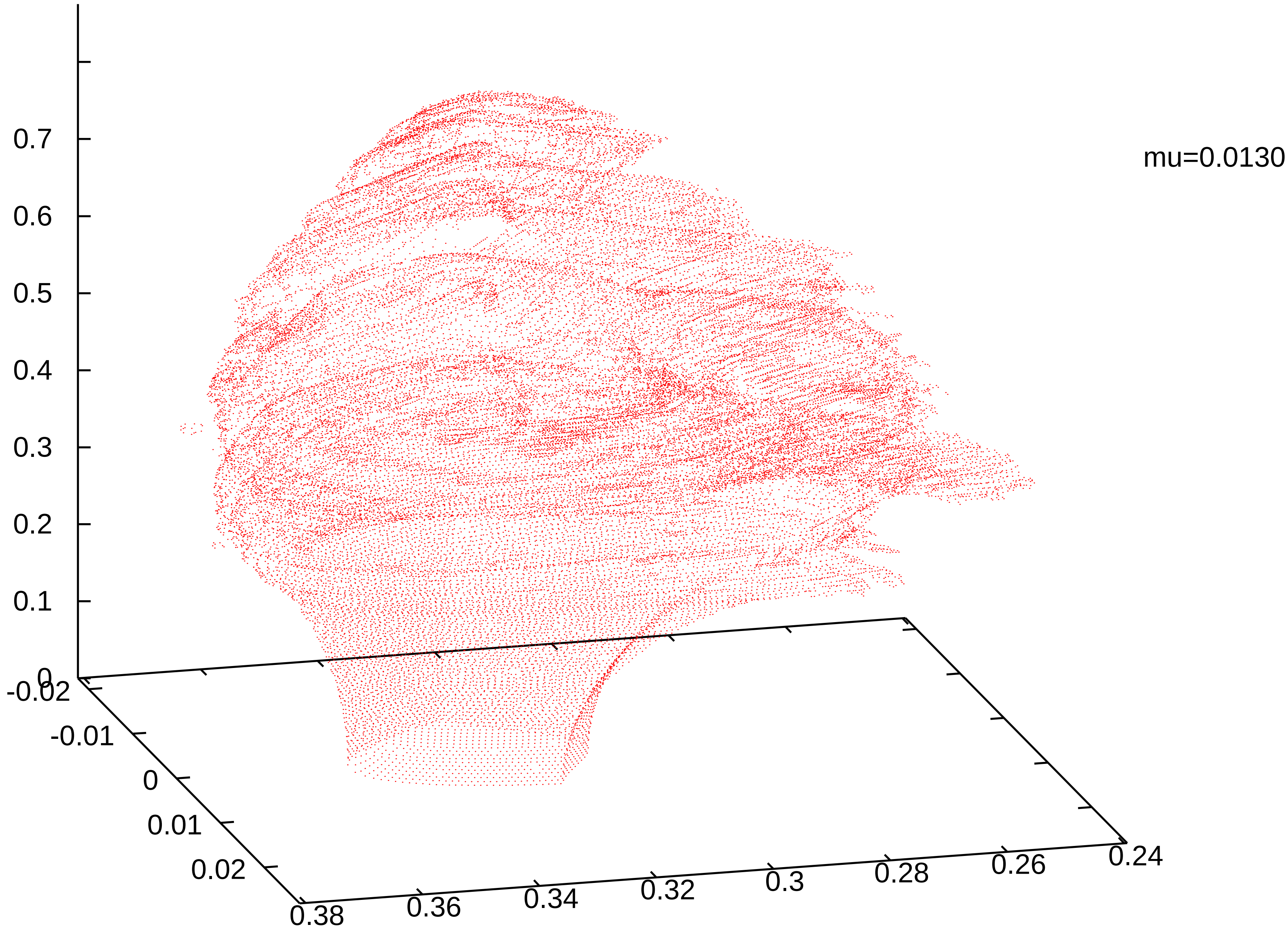

mu=0.0130
0.7
0.6
0.5
0.4
0.3
0.2
0.1
0
-0.02
-0.01
0
0.01
0.02
0.38
0.36
0.34
0.32
0.3
0.28
0.26
0.24

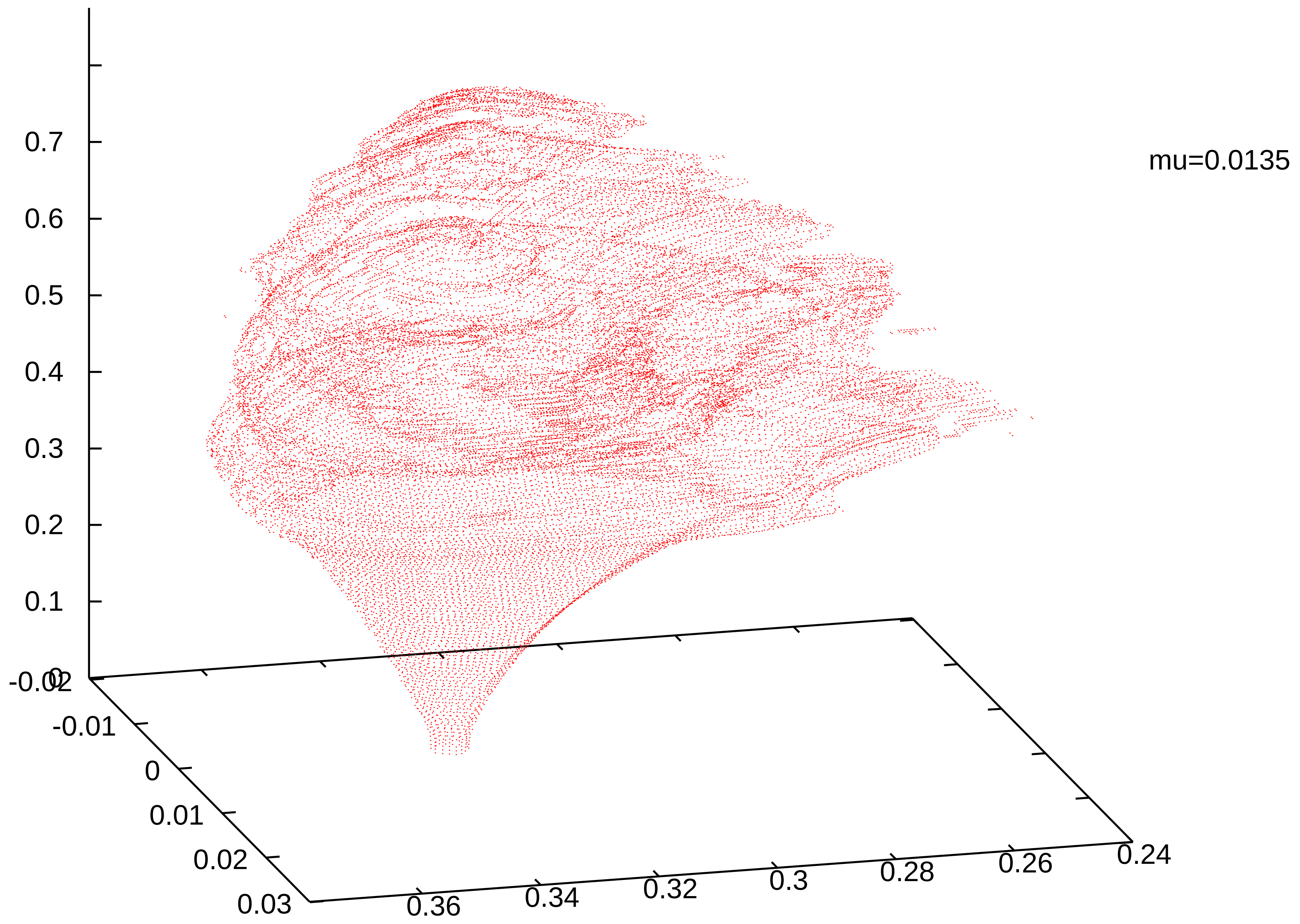

mu=0.0135
0.7
0.6
0.5
0.4
0.3
0.2
0.1
0
-0.02
-0.01
0
0.01
0.02
0.03
0.36
0.34
0.32
0.3
0.28
0.26
0.24

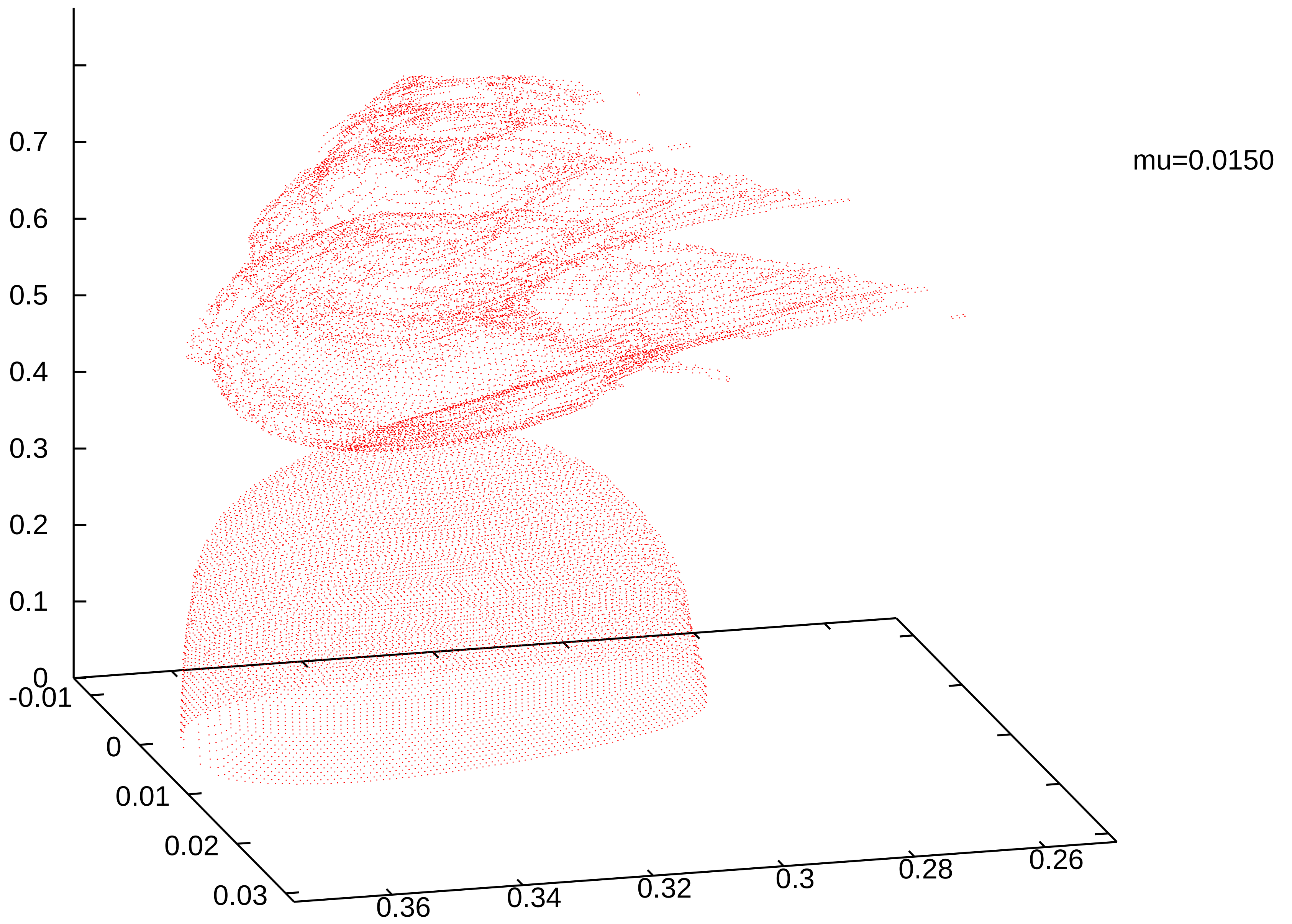

mu=0.0150
0.7
0.6
0.5
0.4
0.3
0.2
0.1
0
-0.01
0
0.01
0.02
0.03
0.36
0.34
0.32
0.3
0.28
0.26

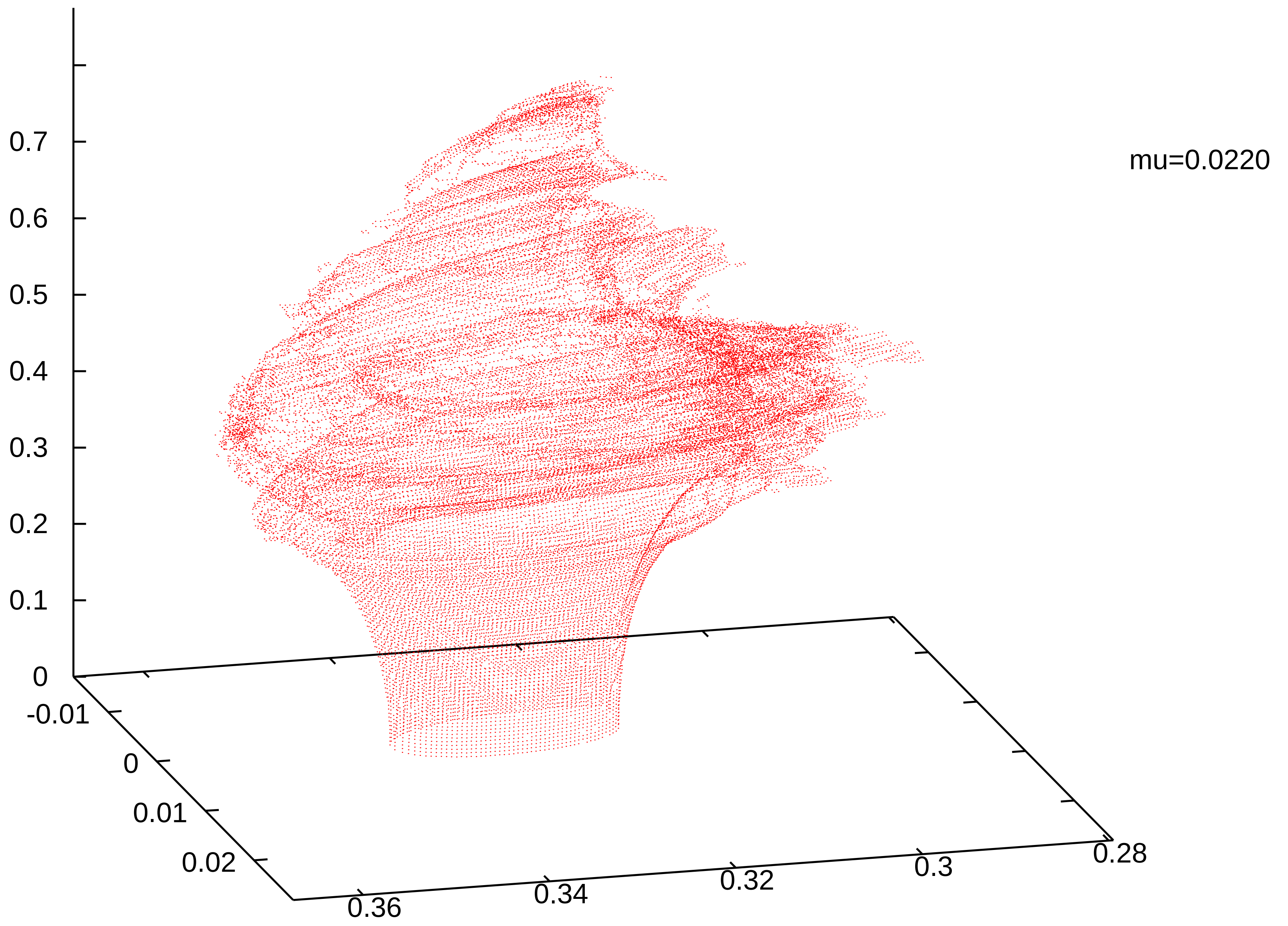

mu=0.0220
0.7
0.6
0.5
0.4
0.3
0.2
0.1
0
-0.01
0
0.01
0.02
0.36
0.34
0.32
0.3
0.28

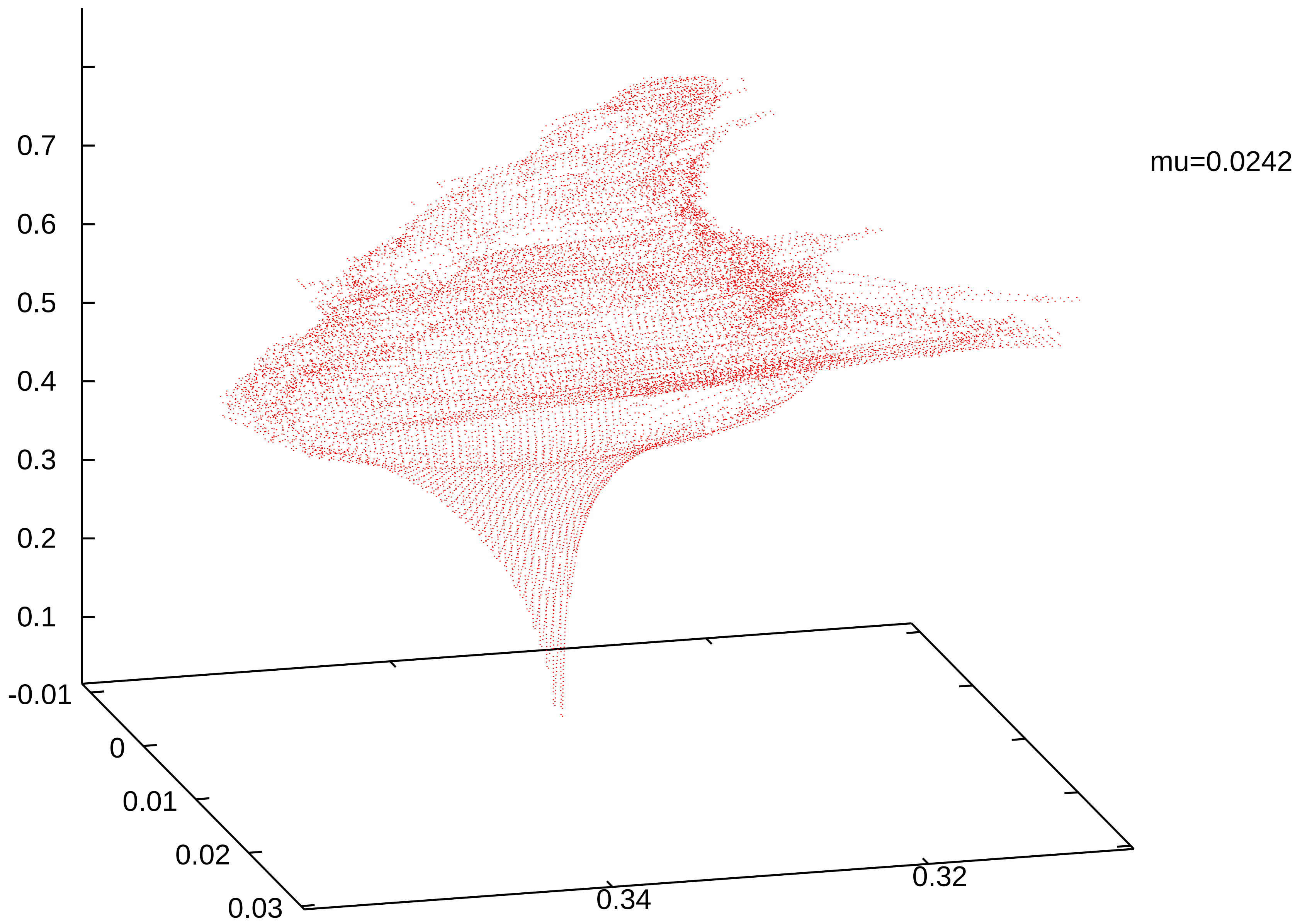
0.7
0.6
0.5
0.4
0.3
0.2
0.1
-0.01
0
0.01
0.02
0.03
0.34
0.32
mu=0.0242

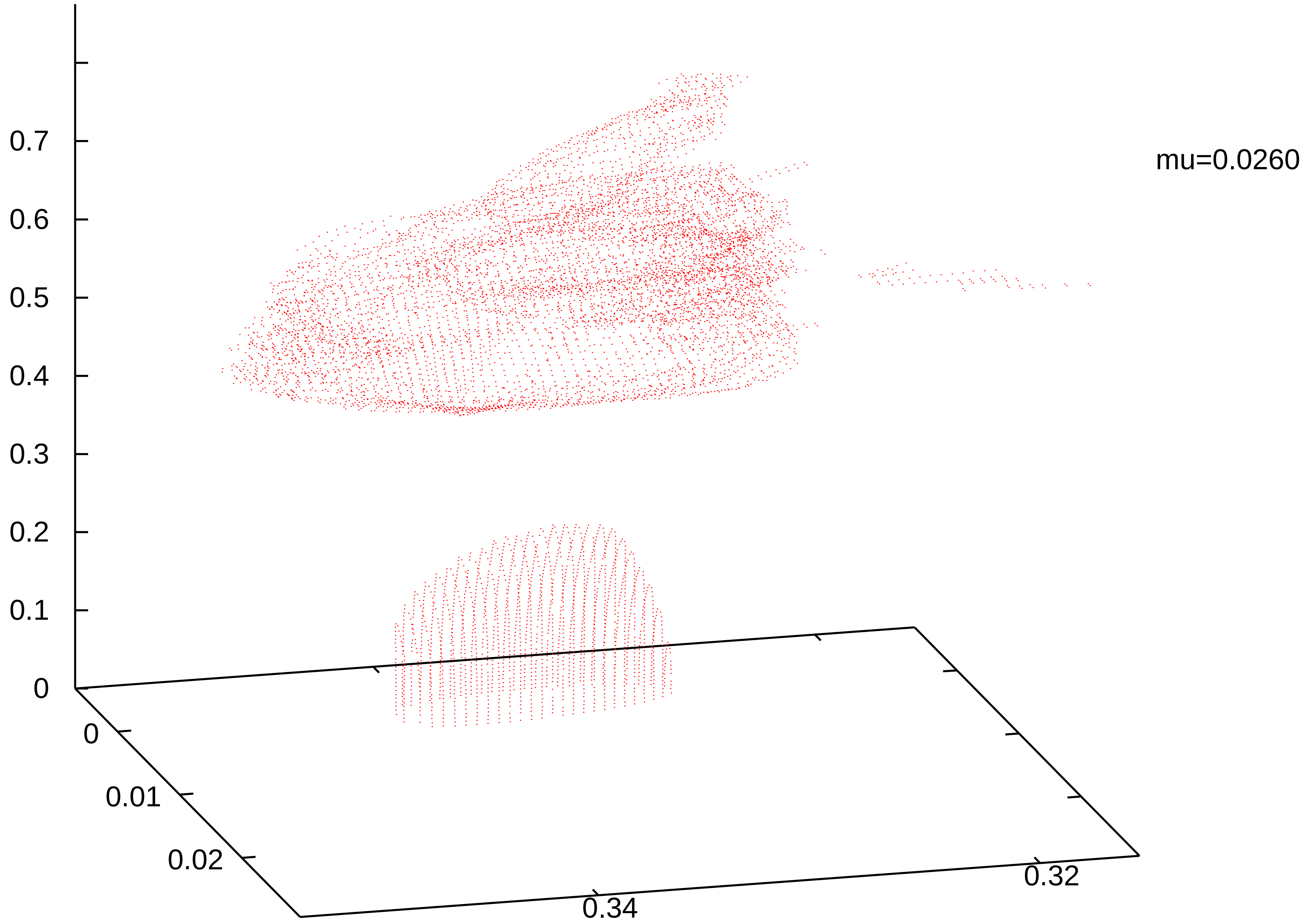

mu=0.0260
0.7
0.6
0.5
0.4
0.3
0.2
0.1
0
0
0.01
0.02
0.34
0.32

Next task is the identification of the different objects which "bound" (in some way) those regions of "numerical practical stability". In general this task becomes increasingly difficult when increasing μ. However some parts of the boundaries are associated to sharp transitions : nearby points escape quickly or remain on the desired region for very long time. In this case the identification becomes easier.

For the moment some of these object are identified as union of stable/unstable manifolds of invariant (normally hyperbolic) tori sitting on the center manifold of the collinear point L_3 or on the center manifold of families of periodic orbits of elliptic-hyperbolic type. The type of a periodic orbit can be seen in any Poincaré section.

All of these objects are codimension 1 and play a key role in many applied sciences.

Still **a lot of work** to be done ...

Other applications

Just to name a few:

- Computation of periodic orbits, invariant tori, invariant manifolds, homo and heteroclinic connections in relatively simple models, requiring a good accuracy,
- Analysis of models depending on several parameters, looking for bifurcations, Lyapunov exponents, in massive simulations, where computing time is relevant,
- Problems where multiple precision is essential: splitting of separatrices for systems not far from integrable, detection of the order of regularity of some phenomena (e.g.: problems of regularisation),
- It has been applied to compute space missions, choreographies, etc.

Final comments

Taylor method is suitable and fast provided the system to be integrated is analytic (or $\mathscr{C}^r$ with r big), with a r.h.s. which is not difficult to evaluate explicitly.

With some caution in the selection of order and truncation error can be as accurate as possible, the main source of error being round off errors.

It seems to be unbeatable when faced to multiprecision.

It is not suitable for stiff systems, systems for which the evaluation of the vector field has to be done by indirect methods (as in some evolution PDE) or for systems whose solutions pass close to singularities which occur for complex time with small imaginary part.